Comparative Transcriptome and WGCNA Reveal Candidate Genes Involved in Petaloid Stamens in Paeonia Lactiflora

Yongming Fan
Beijing Forestry University
Yanyi Zheng
Beijing Forestry University
Jaime A. Teixeira da Silva
Independent
Xiaonan Yu (yuxiaonan626@126.com)
College of Landscape Architecture, Beijing Forestry University, Beijing, 100083, P.R. China;

Research article

Keywords: Comparative transcriptome, Paeonia lactiflora, Petaloid stamens, Trend analysis, Weighted gene coexpression network

Posted Date: October 23rd, 2020

DOI: https://doi.org/10.21203/rs.3.rs-95599/v1

Abstract

Background: The phenomenon of petaloid stamens in *Paeonia lactiflora* is an important cause of double flower formation. Although research on stamen development in model plants has progressed, the molecular mechanism of *P. lactiflora* petaloid stamens is still unclear.

Results: In this study, a comparative transcriptomic analysis was performed on two cultivars of *P. lactiflora* ('Fen Yu Nu' and 'Lian Tai') with different stamen developmental patterns. Using transcriptome sequencing, 89,393 unigenes were identified in *P. lactiflora*. Trend analysis and weighted gene co-expression network analysis (WGCNA) indicated that 18 candidate genes were likely involved in petaloid stamens, including seven MADS-box genes *PlAP3*, *PlDEFA*, *PlPI2*, *PlAG-1*, *PlSEP3*, *PlSEP1-1*, and *PlSEP1-2*, and 11 transcription factors (TFs) *PlTCP2*, *PlTCP4*, *PlTCP9*, *PlbHLH36*, *PlICE1*, *PlLBD38*, *PlNAC083*, *PlBLH11*, *PlPDF2*, *PlGBF1*, and *PlIIIA*. Based on the selected candidate genes, a hypothetical model of gene expression network regulating petaloid stamens is proposed.

Conclusions: Our results provide a collection of candidate genes for the analysis of *P. lactiflora* petaloid stamens, allowing for in-depth studies of the development pattern of *P. lactiflora* flower organs, and providing a theoretical basis for related research on petaloid stamens of other herbaceous flowers.

Background

Among flower forms, double flowers have a huge assortment of flower and petal shapes, and a strong three-dimensional effect [1]. Double flowers have higher ornamental value on the cut flower market than single-petaled flowers, and occupy a larger section of that market [2]. The flower developmental pattern of ornamental plants has always been an important research theme for plant researchers. Double flower breeding is a central goal of all ornamental plant breeding [3, 4]. Petaloid stamens can be described as petal-like stamens without a distinct anther and filament but occasionally with marginal microsporangia. In *Prunus lannesiana*, the number of stamens in double flowers was significantly higher than in single flowers, and the increase in petals might have been caused by petaloid stamens [5]. In Arabidopsis, mutations in the *AGAMOUS* gene cause stamens to transform into petals [6]. In *Camellia japonica*, ectopic expression of *CjAG* in Arabidopsis resulted in an increased number of stamens and reduced petals [7]. These studies show that the increase in petals of double flowers may be caused by petaloid stamens. *Paeonia lactiflora* (Paeoniaceae) is a perennial herbaceous flower with high ornamental value, and a traditional Chinese flower that enjoys the reputation as the 'Prime Minister of flowers' in China [8, 9]. *P. lactiflora* has abundant flower types depending on the flower developmental pattern, and there are 13 flower types in China [10, 11]. Stamen petaloid may be one main method for forming double flowers in herbaceous peony [12, 13]. Breeding and maintaining traits of double flowers is of great importance in herbaceous peony breeding and production programs. Therefore, central to these breeding objectives is an appreciation of how flower type changes by understanding the molecular mechanism regulating the formation of double-petaled flowers.

The ABCDE model and floral quartets of floral organ development are important theoretical foundations for the study of petaloid stamens in herbaceous peony [14–16]. In *Arabidopsis thaliana*, the ABCDE floral organ development model has been continuously developed and perfected. The three types of BCE-class genes are involved in the development of stamens, including *AP3*, *PI*, *AG*, *SEP1*, *SEP2*, *SEP3*, and *SEP4* [17–19]. In *Prunus mume*, *PmSEP1* and *PmSEP4* are involved in the formation of floral meristems, *PmSEP1* and *PmSEP4* are involved in the formation of sepals, *PmSEP2* and *PmSEP3* are involved in the formation of petals, *PmSEP2* and *PmSEP3* are involved in the formation of stamens, and *PmSEP2* and *PmSEP3* are involved in the formation of pistils [20]. In *Triticum aestivum*, Su et al. [21] found that the *TaAGL6* transcription factor (TF) plays an essential role in stamen development through transcriptional regulation of *TaAP3* and other related genes. In rice, the B-class *OsMADS16* gene plays a key role in stamen formation [22]. In *Brassica campestris*, when *BcMF28*, which encodes a R2R3-MYB TF, was overexpressed in Arabidopsis, it caused defects in stamen development, interfering with the phenylalanine metabolic pathway, indicating that *BcMF28* plays an important regulatory role during late stamen development [23]. In *Opithandra*, the complementarity of *OpdcyclinD3* to *OpdCYC* expression shows that *OpdCYC* expression was related to the abortion of dorsal and ventral stamens through negative regulation of the *OpdcyclinD3* gene. In *P. lactiflora*, Gong et al. [24] revealed the possible role of variation in B-class MADS-box gene expression, specifically affecting identity and morphological variation in the corolla. However, an in-depth, comprehensive study on the petaloid stamens of *P. lactiflora* and the regulatory relationship between related genes has not been reported.

Total RNA sequencing (RNA-Seq) is an important method to obtain effective functional genes of non-reference genome species [25, 26]. Weighted gene co-expression network analysis (WGCNA) allows gene expression patterns in multiple samples to be analyzed [27] At present, WGCNA analysis has been combined with transcriptome sequencing to study various aspects of plant science, including flower development [28, 29]. In *Lagerstroemia speciosa*, 73,536 unigenes and 30,714 differently expressed genes (DEGs) were identified by transcriptome sequencing, and four key genes related to petaloid stamens were screened out using WGCNA analysis [30]. In *Dactylis glomerata*, 4689 up-regulated DEGs and 3841 down-regulated DEGs were identified by transcriptome sequencing, and WGCNA analyzed the connection to transcriptional changes at different stages and provided evidence of an internal relationship between modules related to signal transduction, stress response, cell division and hormone transport [31]. In *Chrysanthemum × morifolium*, comparative transcriptomics and WGCNA screened out six TFs (*CmMYB305*, *CmMYB29*, *CmRAD3*, *CmbZIP61*, *CmAGL24*, and *CmNAC1*), revealing the potential regulatory mechanism of carotenoid accumulation [32]. This study is the first attempt to explore the co-expression network relationship between genes related to petaloid stamens of *P. lactiflora*.

There are currently no reports on the molecular mechanism related to petaloid stamens of herbaceous peony. In this study, we used comparative transcriptomics and WGCNA to analyze the trends in gene expression levels in the flower buds of two cultivars of *P. lactiflora* at different developmental stages, and constructed a gene co-expression network. A phylogenetic analysis was performed on selected DEGs and on genes related to stamen development in *A. thaliana*, and finally identified candidate genes related to petaloid stamens of *P. lactiflora*. This study reveals candidate genes that may regulate the development

of petaloid stamens in herbaceous peony, and provides theoretical guidance for the targeted cultivation of herbaceous peony cultivars with various flower types.

Results

Morphological description of flower bud differentiation in P. lactiflora

In this study, two cultivars of *P. lactiflora*, 'Fen Yu Nu' (normal stamens) (Fig. 1A) and 'Lian Tai' (petaloid stamens) (Fig. 1B) were selected to observe their developmental processes. Anatomically, the stamens of FYN followed a normal state of development, and could be divided into S (stamen primordium) (Fig. 1A, A3), S1 (elongated stamen) (Fig. 1A, A4) and S2 (stamens completely developed) (Fig. 1A, A5) while the development of LT stamens could be divided into S (stamen primordium) (Fig. 1B, B3), S1 (stamen partly petaloid) (Fig. 1B, B4) and S2 (stamen completely petaloid) (Fig. 1B, B5). There was a clear difference in the differentiation and development of the stamens in both cultivars. We also observed that the size (area) of flower buds of both FYN and LT increased as flower buds differentiated, but the average size of flower buds at same stage in LT was always larger than that in FYN (Fig. 1A, A1; Fig. 1B, B1). Given that there are differences between FYN and LT in terms of morphology and stamen developmental patterns, these cultivars could serve as ideal test material for subsequent transcriptomics research.

Overview of P. lactiflora 'FYN' and 'LT' mRNA

A total of 52,307,557 clean reads and 7,819,559,089 clean bases were obtained from 18 cDNA libraries, including nine *P. lactiflora* FYN samples (FYN1, FYN2, FYN3) and nine *P. lactiflora* LT samples (LT1, LT2, LT3). Clean reads were obtained from raw reads by removing reads containing an adaptor, reads with a ratio of $N > 10\%$, and low-quality reads. The number of bases with a quality value $Q \leq 20$ accounted for more than 40% of all reads. The Q20 value of all clean reads of samples exceeded 96.63% (Additional file 1, Table S1), indicating that the quality of the sequencing met the requirements for subsequent analysis [33, 34].

De novo assembly of the reads yielded a total of 89,393 unigenes with a mean size of 839 bp (Additional file 1, Table S2). From among all unigenes, 40,951 unigenes were annotated by at least one of the four databases: 40,649, 22,811, 20,480, 14,246 unigenes were annotated to NCBI's Nr, Swiss-Prot protein, COG/KOG, and KEGG databases, respectively with an E-value threshold $< 10^{-5}$ (Additional file 1, Table S3). Furthermore, 5943, 8348, 3699, 10,182, 11,195, 1945, 13,845, 17,634 and 13,897 DEGs could be distinguished from FYN1 vs. FYN2, FYN1 vs. FYN3, FYN2 vs. FYN3, LT1 vs. LT2, LT1 vs. LT3, LT2 vs. LT3, FYN1 vs. LT1, FYN2 vs. LT2 and FYN3 vs. LT3 comparisons, respectively. The number of DEGs in both cultivars increased at first and then decreased as flower buds differentiated. The number of DEGs of both cultivars in the same sample period (FYN1 vs. LT1, FYN2 vs. LT2 and FYN3 vs. LT3) was more than the number of DEGs of the same cultivar in different sample periods (FYN1 vs. FYN2, FYN1 vs. FYN3, FYN2 vs. FYN3, LT1 vs. LT2, LT1 vs. LT3, LT2 vs. LT3), which was consistent with the correlation test between cultivars (Fig. 2). This may be caused by differences in stamen development between the two cultivars,

supporting the conclusion that the DEGs screened in this study could be used for subsequent biological analysis.

According to the heatmap of Pearson's correlations between samples (Fig. 3), most biological repeats between different samples had good correlations, and many correlations between the two cultivars and different groups were significantly different, indicating a significant differential expression of genes between the sampling time nodes.

DEGs trend analysis of LT, and FYN vs. LT combinations

The trend analysis of all DEGs was divided into eight profiles in FYN, eight profiles in LT, and 20 profiles for FYN vs. LT (Fig. 4). Profiles 7, 6, 1 and 0 in LT had significantly enriched patterns. Gene expression levels were up-regulated in modules of profiles 7 and 6. These DEGs could be considered as candidate genes related to petaloid stamens (Fig. 4B). Trend analysis of gene expression levels of FYN and LT showed that seven modules (profiles 0, 2, 7, 16, 17, 18, and 19) showed significantly enriched patterns (Fig. 4C). Some DEGs were expressed in both cultivars, but the expression trends were significantly different. These genes could be used as candidate genes related to petaloid stamens of *P. lactiflora* for further genomic analysis.

In profile 7 of LT, more prominent than in other profiles, the expression of DEGs was continuously up-regulated during the LT1 to LT3 period (Fig. 4B). In profile 7, one GO enrichment (molecular function) was mainly related to oxidoreductase activity, tetrapyrrole binding, iron-sulfur cluster binding, metal cluster binding, and disulfide oxidoreductase activity. KEGG pathways were mainly related to photosynthesis, metabolic pathways, carbon fixation in photosynthetic organisms, photosynthesis-antenna proteins, and glyoxylate and dicarboxylate metabolism (Additional file 2). In profile 7, there were 1669 DEGs. Among them, we screened out one MADS gene (*PlAP3*) and four TFs (*PlPRE6*, *PlRAP2-4*, *PlASIL2*, and *PlGL3*) from three different TF families (Additional file 3).

In profile 6 of LT, the gene expression level of DEGs in the LT2 to LT3 period was higher than in the LT1 period, and the expression level of the DEGs remained high in the LT2 to LT3 period. This expression pattern was highly significant (Fig. 4B). In profile 6, one GO enrichment (molecular function) was mainly related to protein dimerization activity, nucleic acid binding, nucleic acid binding TF activity, tetrapyrrole binding, and protein binding. The KEGG pathways were mainly fatty acid elongation, plant-pathogen interaction, cutin, suberine and wax biosynthesis, brassinosteroid biosynthesis, and biosynthesis of secondary metabolites (Additional file 4). In profile 6, there were 4568 DEGs. Among them, we screened out nine MADS-box genes (*PlAGL2*, *PlAG*, *PlPI2*, *PlAGL8*, *PlDEFA*, *PlSEP1*, *PlAGL6*, *PlSEP3*, and *PlAP1*) and 29 TFs from 11 gene families (Additional file 3).

In profiles 6 and 7, we screened out 11 MADS-box genes and 33 TFs. The expression levels of these genes were significantly different in different sample periods (Fig. 5A).

In profiles 0, 2, 7, 16, 17, 18, and 19, which were significantly enriched by FYN and LT trend analysis, we screened two MADS-box genes (*PlSEP1* and *PlAP3*) and 18 TFs that belonged to 12 TF families (bHLH, AP2/ERF, C2H2, MYB, NAC, Trihelix, LBD, HD-ZIP, TCP, TALE, GRF, and NF-YB) (Additional file 5). In these profiles, all genes were significantly different (Fig. 5B). We screened out DEGs in profiles 16, 17, 18 and 19 that were highly expressed in LT in the FYN vs. LT trend analysis. These genes include two MADS-box genes (*PlSEP1* and *PlAP3*) and 14 TFs (*PlMYC2*, *PlERF114*, *PlDREB2A*, *PlC2H2-like*, *PlTT2-1*, *PlMYB17*, *PlASIL2*, *PlLBD38*, *PlANL2*, *PlTCP11*, *PlBLH2*, *PlBLH11*, *PlGRF1*, and *PlNFYB8*). The genes screened out from the significantly enriched profile could be regarded as candidate genes related to *P. lactiflora* petaloid stamens.

Phylogenetic analysis of DEGs

In the above trend analysis, we screened out 60 DEGs, removed six duplicate genes, and obtained 54 DEGs, including 11 MADS-box genes and 43 TFs. Subsequently, we performed a phylogenetic analysis of the MADS-box genes and TFs with genes related to the regulation of *A. thaliana* stamen development (Additional file 6), and screened out genes that were highly homologous to *A. thaliana* from the DEGs. The results are shown in Fig. 6. We screened a total of six highly homologous MADS-box genes (*PlAP3*, *PlDEFA*, *PlPI2*, *PlAG1*, *PlSEP3*, and *PlSEP1-2*) (Fig. 6A) and eight TFs (*PlLBD38*, *PlTCP2*, *PlTCP4*, *PlTCP9*, *PlNAC083*, *PlbHLH36*, *PlBLH11*, and *PlICE1*) (Fig. 6B).

Division of gene co-expression modules

In order to make the gene distribution conform to the scale-free network, we determined that the power was 8 (Additional file 7). In the module division, the selected TOMType was unsigned, and mergeCutHeight was 0.75 (Fig. 7). DEGs that may be related to petaloid stamens of *P. lactiflora* were clustered into 14 correlated modules. After further analysis, we selected two highly associated modules that may be related to *P. lactiflora* petaloid stamens because the gene expression levels of these two modules continued to increase during LT2 to LT3 periods and were higher than FYN during these periods (Fig. 8).

Weighted correlation network analysis associated with *P. lactiflora* petaloid stamens

In the Ivory module, we screened out two MADS-box genes and 12 TFs from eight TF families (Additional file 8). Cytoscape 3.6.1 software was used to display the network relationships among the selected genes. The gene regulatory network showed connectivity between them. Among them, *PlSEP1-1*, *PlYAB1*, *PlYAB5*, *PlGBF1*, *PlSCL32*, *PlLHY*, *PlANL2* and *PlPDF2* had strong connectivity and could be used as candidate genes for further analysis of genes related to the petaloid stamens of herbaceous peony (Fig. 9A).

In the Brown module, we screened out four TFs from three TF families (Additional file 8). Cytoscape 3.6.1 software was used to display the network relationships among the selected genes. The gene regulatory network showed a connectivity between them. Among them, *PlTCP11*, *PlC2H2-like*, *PlMYC2* and *PlIIIA* had strong connectivity and could be used as candidate genes for further analysis of genes related to *P. lactiflora* petaloid stamens (Fig. 9B).

Finally, we screened a total of 12 DEGs in Ivory and Brown modules with strong connectivity. We conducted a phylogenetic analysis of these genes. The results showed that one MADS-box gene (*PlSEP1-1*) and three TFs (*PlPDF2*, *PlGBF1*, and *PlIIIA*) were highly homologous with *A. thaliana* genes that regulate stamen development (Fig. 10).

Validation Of Deg Expression

In this study, we screened 10 DEGs related to *P. lactiflora* petaloid stamens from the transcriptome, designed specific primers, and performed qRT-PCR verification (Fig. 11; Additional file 9). Our results show that the DEGs showed high expression levels from LT2 to LT3, and that the qRT-PCR and transcriptome sequencing results were consistent (Fig. 5), proving the reliability of transcriptome sequencing results.

Discussion

Study on P. lactiflora **petaloid stamens by comparative transcriptome**

Through comparative transcriptome analysis of two herbaceous cultivars, FYN and LT, we identified six MADS-box genes (*PlAP3*, *PlDEFA*, *PlPI2*, *PlAG-1*, *PlSEP3*, and *PlSEP1-2*) and eight TFs that may be related to the petaloid stamens of *P. lactiflora*. The MADS-box DEGs are consistent with the results of studies in *A. thaliana*. Triple mutant Arabidopsis plants lacking the activity of all three *SEP* genes produce flowers in which all organs develop as sepals, thus *SEP1/2/3* are a class of organ-identity genes that is required for the development of petals, stamens and carpels [35]. The *AP1* gene is required for normal development of sepals and petals, and *SEP3* interacts with AP1 to promote normal flower development in Arabidopsis [36]. In Arabidopsis, floral organs are converted into leaf-like organs in the *sep1*, *sep2*, *sep3*, *sep4* quadruple mutant. *SEP4* also contributes to the development of petals, stamens and carpels, and it plays an important role in the identity of meristems [37]. Mutations in the *AP3* gene of *A. thaliana* result in homeotic transformations of petals to sepals and stamens to carpels [38]. Moreover, in *A. thaliana*, the ABCDE floral organ development model has been continuously developed and perfected. The three types of BCE-class genes are involved in the development of stamens, including *AP3*, *PI*, *AG*, *SEP1*, *SEP2*, *SEP3*, and *SEP4* [15]. In *Oryza sativa*, stamen development is regulated by a BCE-class gene (B-class: *SPW1*, *MADS2* and *MADS4*; C-class: *MADS3* and *MADS58*; E-class: *SEP3*, *MADS7* and *MADS8*), which has a similar regulatory mechanism as Arabidopsis [39]. Based on this, we suspect that the BCE genes in *P. lactiflora* may be the key genes involved in the development of its stamens. Eight TFs from five TF families were identified: TCP (*PlTCP2*, *PlTCP4*, and *PlTCP9*), bHLH (*PlbHLH36*, and *PlICE1*), LBD (*PlLBD38*), NAC (*PlNAC083*), and TALE (*PlBLH11*). TCP family genes were involved in flower development

in Papaveraceae, where TCP/CYC-like (CYL) genes promoted the initiation and growth of stamens, and were also involved in perianth development and specified sepal and petal identity in *Cysticapnos* by regulating the B-class floral organ identity genes [40]. *miR319a* was found to regulate the expression of the *TCP4* gene in *A. thaliana*, leading to severe disruption of petal and stamen development [41]. In this study, we identified three TCP TFs that might be related to the petaloid stamens of *P. lactiflora*: *PlTCP2*, *PlTCP4* and *PlTCP9*. They might have a positive regulatory effect on B-class genes. The JAZ (jasmonate ZIM-domain) proteins represses the bHLH-MYB complex to suppress stamen development and seed production, while jasmonate, a phytohormone, induces JAZ degradation and releases the bHLH-MYB complex to subsequently activate the expression of downstream genes essential for stamen development and seed production [42]. In addition, phylogenetic analysis showed that *PlbHLH36* and *PlICE1* were highly homologous to *AtSUP* and *AtSK11* in *A. thaliana*, respectively, and they were both involved in the development of stamens [43, 44]. Therefore, we suspect that the bHLH family genes *PlbHLH36* and *PlICE1* selected in this study might repress the downstream genes of stamen development, leading to the formation of petaloid stamens. In this study, the results of phylogenetic analysis showed that *PlLBD38* was highly homologous to *AtAFR6* and *AtAFR8* of *A. thaliana. AtAFR6* and *AtAFR8* act redundantly to regulate stamen elongation and flower maturation [45]. Based on this, we speculate that in *P. lactiflora*, *PlLBD38* might regulate the elongation of stamens. *PlNAC083* was highly homologous to *AtNUA* of *A. thaliana*, so *AtNUA* probably acts in the same pathway as ESD4 by affecting flowering time, vegetative and inflorescence development [46]. Therefore, we speculate that it might be involved in nutrient transmission and flower bud development of petaloid stamens in *P. lactiflora*. The function of *PlBLH11* in *P. lactiflora* might be similar to *AtSEP4*, because it was highly homologous to *AtSEP4* in *A. thaliana*.

WGCNA of *P. lactiflora* petaloid stamens

Trend analysis is a commonly used analytical method in transcriptome research. When combined with WGCNA analysis, it can better identify hub genes, i.e., key genes that play a vital role in biological processes. In this study, using WGCNA analyses with *P. lactiflora* and phylogenetic analyses between *P. lactiflora* and *A. thaliana*, we identified a total of one MADS-box gene *SEP1-1* and three TFs (*PlPDF2*, *PlIIIA*, and *PlGBF1*) which had strong connectivity (Fig. 9). Results of phylogenetic analysis showed that *PlPDF2* and *PlIIIA* were highly homologous to *AtSK11* of *A. thaliana* [43]. Therefore, we speculate that *PlPDF2*, *PlIIIA*, *PlbHLH36*, and *PlICE1* might participate in the development of stamens in *P. lactiflora*. *PlGBF1* was highly homologous to *AtJAG* of *A. thaliana*, and in *P. lactiflora*, it might be involved in stamen and carpel development [47, 48].

Inference model of regulatory network of genes for *P. lactiflora* petaloid stamens

Through comparative transcriptomics with WGCNA and phylogenetic analyses, using *A. thaliana*, we inferred a model of gene regulatory network for *P. lactiflora* petaloid stamens (Fig. 12). First, *PlDEFA* and *PlBLH11* are homologous to *AtAP3* and *AtSEP4*, respectively. We speculate that *PlDEFA* and *PlBLH11* are involved in the formation of AP3-PI-AG-SEP class ‘quartet model’, and jointly regulate the development of

stamens in *P. lactiflora* [15]. Then, *PlLBD38* and *PlNAC083* are homologous to *AtARF* and *AtNUA*, respectively. We speculate that they may be involved in stamen elongation and nutrient transmission during stamen development of *P. lactiflora* [45, 46]. Further, we speculate that *PlTCPs*, *PlPDF2*, *PlICE1*, *PlIIIA*, *PlbHLH36*, and *PlGBF1* are likely to be the important regulators in upstream regulatory networks of petaloid stamens in *P. lactiflora* [40, 41, 43, 45, 47, 48]. However, the regulatory network of genes related to *P. lactiflora* petaloid stamens needs further verification.

In the future, the gene regulatory network could be verified from three angles: target gene-protein interaction, protein-protein interaction, and gene function verification. Among them, the main methods of target gene-protein interaction include chromatin immunoprecipitation [49], the gel electrophoretic mobility shift assay [50], foot-printing [51], and the yeast one-hybrid system [52]; the main protein-protein interaction methods include the yeast two-hybrid system [53], bimolecular fluorescence complementation [54], GST-pull down technology [55]; functional verification mainly includes mutant phenotype analysis [56, 57], and GUS staining [58].

Conclusions

Through a comparative transcriptome and WGCNA analysis of two *P. lactiflora* cultivars, FYN and LT, we identified seven MADS-box genes (*PlAP3*, *PlDEFA*, *PlPI2*, *PlAG-1*, *PlSEP3*, *PlSEP1-1*, and *PlSEP1-2*) and 11 TFs (*PlTCP2*, *PlTCP4*, *PlTCP9*, *PlbHLH36*, *PlICE1*, *PlLBD38*, *PlNAC083*, *PlBLH11*, *PlPDF2*, *PlGBF1*, and *PlIIIA*). These genes showed a clear regulatory network for *P. lactiflora* petaloid stamens, paving a clearer understanding of its molecular mechanism. Furthermore, transcriptome sequencing technology and WGCNA analysis provide a theoretical basis for mining the hub genes of *P. lactiflora* petaloid stamens. The results of this study provide useful information for exploring the molecular mechanism of petaloid stamens of herbaceous peony. Petaloid stamens are closely related to the ornamental and commercial value of herbaceous peony, so this study has practical significance for the cultivation of double-flowered herbaceous peony cultivars.

Materials And Methods

Collection of plant materials

The experimental materials were the terminal flower buds of three-year-old *P. lactiflora* ‘Fen Yu Nu’ (FYN) and ‘Lian Tai’ (LT), which were collected from the research field of the Germplasm Resources Nursery of the National Engineering Research Center for Floriculture (116°39'E, 40°17'N, Beijing, China). From February to May 2018, plants were sampled every 5 days, and 5 to 10 flower buds of similar size were taken at each stage, and fixed in FAA (38% formaldehyde (5 mL); glacial acetic acid (5 mL); 50% ethyl alcohol (90 mL)). The stages of flower bud differentiation were determined under a stereomicroscope (Leica EZ4HD, Wetzlar, Germany). Finally, three stages of flower buds, FYN1 (Fig. 1A, A3), FYN2 (Fig. 1A, A4), FYN3 (Fig. 1A, A5) for FYN, and LT1 (Fig. 1B, B3), LT2 (Fig. 1B, B4), LT3 (Fig. 1B, B5) for LT, were selected as research material. Approximately 10 flower buds of similar size were used as biological

replicates at each stage, and three biological samples were collected. The length and diameter of each flower bud were measured with a vernier caliper, and the length × diameter were calculated as the longitudinal section area [29]. Samples were frozen immediately in liquid nitrogen and stored at -80 °C to extract total RNA.

Rna Extraction, Database Construction, Sequel And Illumina Sequencing

Total RNA was extracted from FYN and LT flower buds with Trizol (Life Technologies, Foster City, CA, USA). To assess RNA integrity, 5 μL of each total RNA sample was assessed by 1% Tris-acetic acid-EDTA (TAE) agarose gel electrophoresis while 1 μL of each total RNA sample was assessed using a NanoDrop ND2000 (Thermo Fisher Scientific, Waltham, MA, USA), such that $2.05 < A_{260}/A_{280} < 2.1$, 28S/18S > 1.5, and RNA concentration ≥ 500 ng/μL. After total RNA was extracted, it was reverse transcribed into cDNA using the GoScript™ Reverse Transcription System (Promega, Madison, WI, USA) according to the manufacturer's instructions. cDNA fragments were purified with the QiAquick PCR extraction kit (QiAGEN, Dusseldorf, Germany). The sizes of ligation products were selected by agarose gel electrophoresis, amplified by PCR, and sequenced by Gene Denovo Biotechnology Co. (Guangzhou, China) using Illumina HiSeq™ 4000.

Differentially expressed genes: selection, function annotation, trends analysis and WGCNA

To identify DEGs across samples or groups, the EdgeR package in R software (http://www.r-project.org/) was used. We classified genes with a |log2 fold change (FC)|>1 and a false discovery rate (FDR) < 0.05 as being significant DEGs [59]. DEGs were imported into the Gene Ontology (GO) database (http://www.geneontology.org/) and the web-based ReviGO software (http://revigo.irb.hr) was used to identify GO functional categories ($p < 0.05$) associated with each set of compared samples [60]. Moreover, DEGs were imported into the Kyoto Encyclopedia of Genes and Genomes (KEGG) database (http://www.genome.jp/kegg) to perform significant enrichment analysis of pathways using KOBAS 2.0 software [61]. DEGs were also annotated in the NCBI non-redundant protein (Nr) database (https://ftp.ncbi.nlm.nih.gov/blast/db/FASTA/), COG/KOG database (http://www.ncbi.nlm.nih.gov/COG), and Swiss-Prot protein database (http://www.ebi.ac.uk/swissprot/).

Trend analysis of each cultivar at different periods used gene expression levels as data for analysis. In order to check the expression pattern of DEGs, the trend analysis between both cultivars first normalized the expression data of each sample (in the order of processing) to 0, log2 (LT1/FYN1), log2 (LT2/FYN2), and log2 (LT3/FYN3), then Short Time-series Expression Miner (STEM) software (http://www.cs.cmu.edu/~jernst/stem/) was used to analyze differential gene clustering patterns [62]. The R package heatmap was used to draw the heatmap. MEGA7 software (https://www.megasoftware.net/) was used to draw the phylogenetic tree.

Co-expression networks were constructed using the WGCNA (v1.47) package in R software [63]. Before performing WGCNA analysis, selected gene sets were filtered to remove low-quality genes. For an unsigned network, the correlation coefficient between gene i and j was defined as Sij: Sij = |cor(i,j)|. Then, to determine the soft thresholding power according to the principle of a non-scale network, the smallest power value when the correlation coefficient reached the plateau period was used as the parameter for subsequent analysis. Moreover, a topological matrix was created using the topological overlap measure (TOM), and the genes were hierarchically clustered based on topological matrix similarity [64, 65]. A gene cluster tree was constructed based on the correlation between gene expression levels, a dynamic hybrid cutting method was used to identify co-expressed gene modules: the minimum number of modules (minModuleSize) was set to 50 genes and then, according to the similarity of the module feature values, the modules with similar expression patterns were merged (mergeCutHeight) [66].

Construction Of A Gene Interaction Network

Gene connectivity within a module represents the regulatory relationship between a gene and other genes. The higher the connectivity, the greater the regulatory role of the gene in the module, and the more likely it is to be a potential hub gene [67]. We screened the top 10 genes in the connectivity of each module, and then selected genes with a cut-off of the weight parameter weight value > 0.2 (the gene weight value of the Ivory module was set to 0.3) and gene connection numbers > 5 as candidate genes for the construction of a gene interaction network [29, 68, 69]. Cytoscape 3.6.1 software (https://cytoscape.org) was used to display the regulatory relationship of DEGs between modules [70].

Qrt-pcr Verification

Quantitative real-time PCR (qRT-PCR) was performed on DEGs selected by trend analysis and WGCNA analysis. cDNA reverse transcribed using the GoScript™ Reverse Transcription System (Promega) was used as template and SYBR Green SuperMix Plus (Novoprotein Technology Co. Ltd., Shanghai, China) served as the fluorescent dye. The primers were designed on the Integrated DNA Technologies website (https://sg.idtdna.com). Primers were synthesized by Beijing Ruibo Xingke Biotechnology Co. Ltd. (Beijing, China). The reaction system was 20 μL, including 10 μL of 2 × NovoStart® SYBR qPCR SuperMix Plus, 1.0 μL of each primer, 7.0 μL of RNase-free water, and 1 μL of template. The PCR cycle was: 1 min at 95 °C, 40 cycles of 20 s at 95 °C, 20 s at 55 °C, and 30 s at 72 °C. A Bio-Rad CFX96™ Real-Time System (Bio-Rad, Hercules, CA, USA) was used for qRT-PCR, each reaction was performed with three biological replicates and relative gene expression levels were calculated according to the $2^{-\Delta\Delta Ct}$ comparative threshold cycle (Ct) method [71].

Abbreviations

P. lactiflora

Paeonia lactiflora; *A. thaliana*:*Arabidopsis thaliana*; DEGs:Differentially expressed genes; FYN:Fen Yu Nu; LT:Lian Tai; WGCNA:Weighted gene co-expression network analysis; TFs:Transcription factors; GO:Gene ontology; KEGG:Kyoto Encyclopedia of Genes and Genomes; qRT-PCR:Quantitative real-time PCR; FYN1:stamen primordium period of Fen Yu Nu; LT1:stamen primordium period of Lian Tai; FYN2:stamens elongated period of Fen Yu Nu; LT2:stamens partly petaloid period of Lian Tai; FYN3:stamens complete development period of Fen Yu Nu; LT3:stamens complete petaloid period of Lian Tai; AP1:APETALA1; SEP:SEPALLATA; AG:AGAMOUS; AGL:AGAMOUS-like;

Declarations

Acknowledgments

Not applicable.

Funding

This project was supported by the Forestry science and technology development project from State Forestry and Grassland Administration (KJZXZZ2019001) and the World-Class Discipline Construction and Characteristic Development Guidance Funds for Beijing Forestry University (2019XKJS0322)

Availability of data and materials

All relevant supplementary data is provided within this manuscript as Additional files 1, 2, 3, 4, 5, 6, 7, 8 and 9. The sequence raw data from this study have been submitted to the NCBI Sequence Read Archive (PRJNA663282).

Authors' contributions

YF wrote the article; YZ provided assistance in qRT-PCR and helped with the literature review; JATS and XY offered critical analysis and supervision, and edited re-wrote and revised all versions of the manuscript.

Ethics approval and consent to participate

Not applicable

Consent for publication

Not applicable.

Competing interests

The authors declare that they have no competing

Publisher's Note

Springer Nature remains neutral with regard to jurisdictional claims in published maps and institutional affiliations.

References

1. Kramer EM, Lenhard M. Shape and form in plant development. Semin Cell Dev Biol. 2018; 79: 1-2.
2. Gattolin S, Cirilli M, Pacheco I, Ciacciulli A, Da Silva Linge C, Mauroux JB, Lambert P, Cammarata E, Bassi D, Pascal T, Rossini L. Deletion of the miR172 target site in a TOE-type gene is a strong candidate variant for dominant double-flower trait in Rosaceae. Plant J. 2018; 96(2): 358-371.
3. Irish VF. The flowering of Arabidopsis flower development. Plant J. 2010, 61: 1014-1028.
4. Thomson B, Wellmer F. Molecular regulation of flower development. Curr Top Dev Biol. 2019; 131: 185-210.
5. Liu Z, Zhang D, Liu D, Li F, Lu H. Exon skipping of AGAMOUS homolog PrseAG in developing double flowers of Prunus lannesiana (Rosaceae). Plant Cell Rep. 2013; 32(2): 227-237.
6. Dennis L, Peacock J. Genes directing flower development in Arabidopsis. Plant Cell. 2019; 31(6): 1192-1193.
7. Sun Y, Fan Z, Li X, Liu Z, Li J, Yin H. Distinct double flower varieties in Camellia japonica exhibit both expansion and contraction of C-class gene expression. BMC Plant Biol. 2014; 14: 288.
8. Fan Y, Wang Q, Dong Z, Yin Y, Teixeira da Silva JA, Yu X. Advances in molecular biology of Paeonia L. Planta. 2020; 251: 23.
9. Yang Y, Sun M, Li S, Chen Q, Teixeira da Silva JA, Wang A, Yu XN, Wang LS. Germplasm resources and genetic breeding of Paeonia: a systematic review. Hortic Res. 2020; 7: 107.
10. Yu XN. Herbaceous Peonies. China Forestry Publishing House, 2019.
11. Zhang JJ, Zhu W, Teixeira da Silva JA, Fan YM, Yu XN. Comprehensive application of different methods of observation provides new insight into flower bud differentiation of double-flowered Paeonia lactiflora ‘Dafugui. HortScience. 2019; 54(1): 28-37.
12. Qin KJ, Li JY. Research on flower type classification of tree peony and herbaceous peony. Journal of Beijing Forestry University. 1990; 1: 18-26. **(in Chinese)**
13. Wang ZZ, Zhang YX. A Discussion on the formation and evolution of flower type of tree peony and herbaceous peony by observing flower bud differentiation of herb peony. Acta Hortic Sin. 1991; 2: 163-168+193-194. **(in Chinese with English abstract)**
14. Coen ES, Meyerowitz EM. The war of the whorls: genetic interactions controlling flower development. Nature. 1991; 353: 31-37.
15. Theissen G, Saedler H. Plant biology. Floral quartets. Nature. 2001; 409(6819): 469-471.
16. Wang Y, Li Y, Yan X, Ding L, Shen L, Yu H. Characterization of C- and D-class MADS-box genes in orchids. Plant Physiol. 2020; 00487.
17. Pelaz S, Ditta GS, Baumann E, Wisman E, Yanofsky MF. B and C floral organ identity functions require SEPALLATA MADS-box genes. Nature. 2000; 405: 200-203.
18. Pelaz S, Gustafson-Brown C, Kohalmi SE, Crosby WL, Yanofsky MF. APETALA1 and SEPALLATA3 interact to promote flower development. Plant J. 2001; 26(4): 385-394.

19. Ditta G, Pinyopich A, Robles P, Pelaz S, Yanofsky MF. The SEP4 gene of Arabidopsis thaliana functions in floral organ and meristem identity. Curr Biol. 2004; 14(21): 1935-1940.
20. Zhou Y, Xu Z, Yong X, Ahmad S, Yang W, Cheng T, Wang J, Zhang Q. SEP-class genes in Prunus mume and their likely role in floral organ development. BMC Plant Biol. 2017; 17(1): 10.
21. Su Y, Liu J, Liang W, Dou Y, Fu R, Li W, Feng C, Gao C, Zhang D, Kang Z, Li H. Wheat AGAMOUS LIKE 6 transcription factors function in stamen development by regulating the expression of Ta APETALA3. Development. 2019; 146(20): dev177527.
22. Kong L, Duan Y, Ye Y, Cai Z, Wang F, Qu X, Qiu R, Wu C, Wu W. Screening and analysis of proteins interacting with OsMADS16 in rice (Oryza sativa L.). PLoS ONE. 2019; 14(8): e0221473.
23. Shen X, Hu Z, Xiang X, Xu L, Cao J. Overexpression of a stamen-specific R2R3-MYB gene BcMF28 causes aberrant stamen development in transgenic Arabidopsis. Biochem Biophys Res Commun. 2019; 518(4): 726-731.
24. Gong P, Ao X, Liu G, Cheng F, He C. Duplication and whorl-specific down-regulation of the obligate AP3-PI heterodimer genes explain the origin of Paeonia lactiflora plants with spontaneous corolla mutation. Plant Cell Physiol. 2017; 58(3): 411-425.
25. Yue J, Zhu C, Zhou Y, Niu X, Miao M, Tang X, Chen F, Zhao W, Liu Y. Transcriptome analysis of differentially expressed unigenes involved in flavonoid biosynthesis during flower development of Chrysanthemum morifolium 'Chuju'. Sci Rep. 2018; 8(1): 13414.
26. Wang T, Yang B, Guan Q, Chen X, Zhong Z, Huang W, Zhu W, Tian J. Transcriptional regulation of Lonicera japonica Thunb. during flower development as revealed by comprehensive analysis of transcription factors. BMC Plant Biol. 2019; 19(1): 198.
27. Langfelder P, Horvath S. WGCNA: an R package for weighted correlation network analysis. BMC Bioinformatics. 2008; 9(1): 559.
28. Yang Y, Bao S, Zhou X, Liu J, Zhuang Y. The key genes and pathways related to male sterility of eggplant revealed by comparative transcriptome analysis. BMC Plant Biol. 2018; 18(1): 209.
29. Liu N, Cheng F, Zhong Y, Guo X. Comparative transcriptome and coexpression network analysis of carpel quantitative variation in Paeonia rockii. BMC Genomics. 2019; 20(1): 683.
30. Hu L, Zheng T, Cai M, Pan H, Wang J, Zhang Q. Transcriptome analysis during floral organ development provides insights into petaloid stamens in Lagerstroemia speciosa. Plant Physiol Biochem. 2019; 142: 510-518.
31. Feng G, Huang L, Li J, Wang JP, Xu L, Pan L, Zhao XX, Wang X, Huang T, Zhang XQ. Comprehensive transcriptome analysis reveals distinct regulatory programs during vernalization and floral bud development of orchardgrass (Dactylis glomerata L.). BMC Plant Biol. 2017; 17(1): 216.
32. Lu C, Pu Y, Liu Y, Li Y, Qu J, Huang H, Dai S. Comparative transcriptomics and weighted gene co-expression correlation network analysis (WGCNA) reveal potential regulation mechanism of carotenoid accumulation in Chrysanthemum × morifolium. Plant Physiol Biochem. 2019; 142: 415-428.

33. Wu Y, Ma Y, Hu S, Zhao B, Yang W, Sun Z, Zhu B, Lu Y, Li P, Du S. Transcriptomic-proteomics-anticoagulant bioactivity integrated study of Pheretima guillemi. J Ethnopharmacol. 2019; 243: 112101.
34. Ye W, Wu H, He X, Wang L, Zhang W, Li H, Fan Y, Tan G, Liu T, Gao X. Transcriptome sequencing of chemically induced Aquilaria sinensis to identify genes related to agarwood formation. PLoS ONE. 2016; 11(5): e0155505.
35. Pelaz S, Ditta GS, Baumann E, Wisman E, Yanofsky MF. B and C floral organ identity functions require SEPALLATA MADS-box genes. Nature. 2000; 405: 200-203.
36. Pelaz S, Gustafson-Brown C, Kohalmi SE, Crosby WL, Yanofsky MF. APETALA1 and SEPALLATA3 interact to promote flower development. Plant J. 2001; 26(4): 385-394.
37. Ditta G, Pinyopich A., Robles P, Pelaz S, Yanofsky MF. The SEP4 gene of Arabidopsis thaliana functions in floral organ and meristem identity. Curr Biol. 2004; 14(21): 1935-1940.
38. Jack T, Brockman LL, Meyerowitz EM. The homeotic gene APETALA3 of Arabidopsis thaliana encodes a MADS box and is expressed in petals and stamens. Cell. 1992; 68: 683–697.
39. Yoshida H, Nagato Y. Flower development in rice. J Exp Bot. 2011; 62(14): 4719-4730.
40. Zhao Y, Pfannebecker K, Dommes AB, Hidalgo O, Becker A, Elomaa P. Evolutionary diversification of CYC/TB1-like TCP homologs and their recruitment for the control of branching and floral morphology in Papaveraceae (basal eudicots). New Phytol. 2018; 220(1): 317-331.
41. Nag A, King S, Jack T. miR319a targeting of TCP4 is critical for petal growth and development in Arabidopsis. Proc Natl Acad Sci USA. 2009; 106(52): 22534-22539.
42. Qi T, Huang H, Song S, Xie D. Regulation of jasmonate-mediated stamen development and seed production by a bHLH-MYB complex in Arabidopsis. Plant Cell. 2015; 27(6): 1620-1633.
43. Dornelas MC, Van Lammeren AA, Kreis M. Arabidopsis thaliana SHAGGY-related protein kinases (AtSK11 and 12) function in perianth and gynoecium development. Plant J. 2000; 21(5): 419-429.
44. Xu Y, Prunet N, Gan ES, Wang YB, Stewart D, Wellmer F, Huang JB, Yamaguchi N, Tatsumi Y, Kojima M, Kiba T, Sakakibara H, Jack TP, Meyerowitz EM, Ito T. SUPERMAN regulates floral whorl boundaries through control of auxin biosynthesis. EMBO J. 2018; 37(11): e97499.
45. Ghelli R, Brunetti P, Napoli N, De Paolis A, Cecchetti V, Tsuge T, Serino G, Matsui M, Mele G, Rinaldi G, Palumbo GA, Barozzi F, Costantino P, Cardarelli M. A newly identified flower-specific splice variant of AUXIN RESPONSE FACTOR8 regulates stamen elongation and endothecium lignification in Arabidopsis. Plant Cell. 2018; 30(3): 620-637.
46. Xu XM, Rose A, Muthuswamy S, et al. NUCLEAR PORE ANCHOR, the Arabidopsis homolog of Tpr/Mlp1/Mlp2/megator, is involved in mRNA export and SUMO homeostasis and affects diverse aspects of plant development. Plant Cell. 2007; 19(5): 1537-1548.
47. Dinneny JR, Weigel D, Yanofsky MF. NUBBIN and JAGGED define stamen and carpel shape in Arabidopsis. Development. 2006; 133(9): 1645-1655.

48. Xu B, Li Z, Zhu Y, Wang H, Ma H, Dong A, Huang H. Arabidopsis genes AS1, AS2, and JAG negatively regulate boundary-specifying genes to promote sepal and petal development. Plant Physiol. 2008; 146(2): 566-575.
49. Heyndrickx KS, Van de Velde J, Wang C, Weigel D, Vandepoele K. A functional and evolutionary perspective on transcription factor binding in Arabidopsis thaliana. Plant Cell. 2014; 26(10): 3894-3910.
50. Zhong R, Richardson EA, Ye ZH. The MYB46 transcription factor is a direct target of SND1 and regulates secondary wall biosynthesis in Arabidopsis. Plant Cell. 2007; 19(9): 2776-2792.
51. Carles C, Bies-Etheve N, Aspart L, Léon-Kloosterziel KML, Koornneef M, Echeverria M, Delseny M. Regulation of Arabidopsis thaliana Em genes: role of ABI5. Plant J. 2002; 30(3): 373-383.
52. Wang MM, Reed RR. Molecular cloning of the olfactory neuronal transcription factor Olf-1 by genetic selection in yeast. Nature. 1993; 364(6433): 121-126.
53. Dray E, Siaud N, Dubois E, Doutriaux MP. Interaction between Arabidopsis Brca2 and its partners Rad51, Dmc1, and Dss1. Plant Physiol. 2006; 140(3): 1059-1069.
54. Zhang Y, Liu Z, Wang X, Wang J, Fan K, Li Z, Lin W. DELLA proteins negatively regulate dark-induced senescence and chlorophyll degradation in Arabidopsis through interaction with the transcription factor WRKY6. Plant Cell Rep. 2018; 37(7): 981-992.
55. Li D, Li Y, Zhang L, Wang XY, Zhao Z, Tao ZW, Wang JM, Wang J, Lin M, Li XF, Yang Y. Arabidopsis ABA receptor RCAR1/PYL9 interacts with an R2R3-type MYB transcription factor, AtMYB44. Int J Mol Sci. 2014; 15(5): 8473-8490.
56. Shim JS, Jung C, Lee SJ,, Min KH, Lee YW, Choi YH, Lee JS, Song JT, Kim JK, Choi YD. AtMYB44 regulates WRKY70 expression and modulates antagonistic interaction between salicylic acid and jasmonic acid signaling. Plant J. 2013; 73(3): 483-495.
57. Meng X, Yu H, Zhang Y, Zhuang F, Song X, Gao S, Gao C, Li J. Construction of a genome-wide mutant library in rice using CRISPR/Cas9. Mol Plant. 2017; 10(9): 1238-1241.
58. Cunillera N, Boronat A, Ferrer A. Spatial and temporal patterns of GUS expression directed by 5' regions of the Arabidopsis thaliana farnesyl diphosphate synthase genes FPS1 and FPS2. Plant Mol Biol. 2000; 44(6): 747-758.
59. Benjamini Y, Yekutieli D. The control of the false discovery rate in multiple testing under dependency. Ann Statistics. 2001; 29: 1165-1188.
60. Supek F, Bošnjak M, Škunca N, Šmuc T. REVIGO summarizes and visualizes long lists of gene ontology terms. PLoS ONE. 2011; 6(7): e21800.
61. Xie C, Mao X, Huang J, Ding Y, Wu J, Dong S, Kong L, Gao G, Li C, Wei L. KOBAS 2.0: a web server for annotation and identification of enriched pathways and diseases. Nucleic Acids Res. 2011; 39 (Web Server issue): W316-W322.
62. Ernst J, Bar-Joseph Z. STEM: a tool for the analysis of short time series gene expression data. BMC Bioinformatics. 2006; 7: 191.

63. Langfelder P, Horvath S. WGCNA: an R package for weighted correlation network analysis. BMC Bioinformatics. 2008; 9(1): 559.
64. Li A, Horvath S. Network neighborhood analysis with the multi-node topological overlap measure. Bioinformatics. 2007; 23(2): 222-231.
65. Yip AM, Horvath S. Gene network interconnectedness and the generalized topological overlap measure. BMC Bioinformatics. 2007; 8: 22.
66. Langfelder P, Zhang B, Horvath S. Defining clusters from a hierarchical cluster tree: the Dynamic Tree Cut package for R. Bioinformatics. 2008; 24(5): 719-720.
67. Ma J, Cao YY, Wang LF, Li JJ, Wang H, Fan YP, Li HY. Identification of gene co-expression modules of maize plant height and ear height by WGCNA. Acta Agron Sin. 2020; 1-12. **(in Chinese with English abstract)**
68. Zhu M, Xie H, Wei X, Dossa K, Yu Y, Hui S, Tang G, Zeng X, Yu Y, Hu P, Wang J. WGCNA analysis of salt-responsive core transcriptome identifies novel hub genes in rice. Genes (Basel). 2019; 10(9): 719.
69. Zhang A, Zhang Q, Li J, Gong H, Fan X, Yang Y, Liu X, Yin X. Transcriptome co-expression network analysis identifies key genes and regulators of ripening kiwifruit ester biosynthesis. BMC Plant Biol. 2020; 20(1): 103.
70. Shannon P, Markiel A, Ozier O, Baliga NS, Wang JT, Ramage D, Amin N, Schwikowski B, Ideker T. Cytoscape: a software environment for integrated models of biomolecular interaction networks. Genome Res. 2003; 13(11): 2498-2504.
71. Schmittgen T D, Livak K J. Analyzing real-time PCR data by the comparative C(T) method. Nat. Protoc. 2008; 36: 1101-1108.

Figures

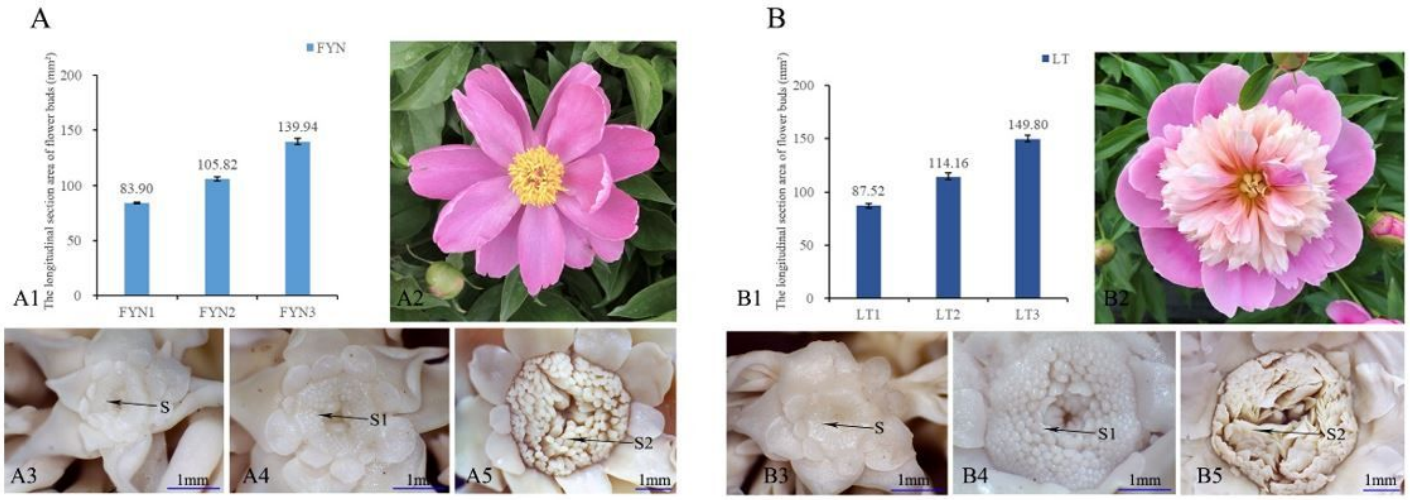

Figure 1

The size of flower buds and material collection stages. A P. lactiflora ‘Fen Yu Nu’ (FYN). B P. lactiflora ‘Lian Tai’ (LT). A1, B1 The longitudinal section area of each flower bud was expressed as the product of its length and diameter. A3, A4, A5 Three-stage flower buds FYN1, FYN2, FYN3; B3, B4, B5 Three-stage flower buds LT1, LT2, LT3. S: stamen primordium period; S1: stamens elongated (FYN) or stamens partly petaloid (LT) period; S2: stamen completed development (FYN) or stamens complete petaloid (LT) period; FYN1, LT1: stamen primordium period; FYN2, LT2: stamens elongated (FYN) or stamens partly petaloid (LT) period; FYN3, LT3: stamens complete development (FYN) or stamens complete petaloid (LT) period.

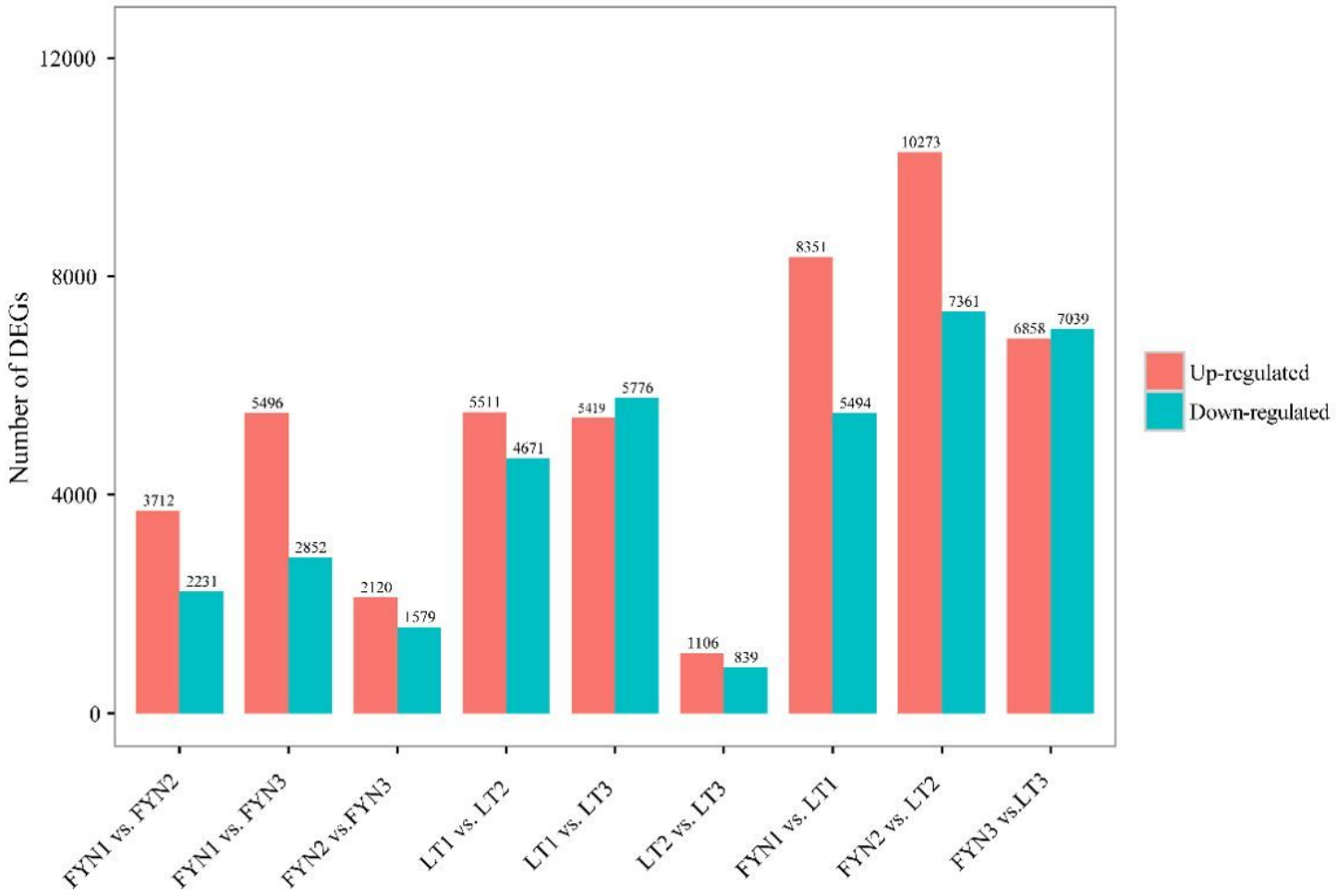

Figure 2

Number of differentially expressed genes (DEGs) between different samples. FYN1, LT1: stamen primordium stage; FYN2, LT2: stamen elongated (FYN) or stamen partly petaloid (LT) stage; FYN3, LT3: stamens complete development or stamen complete petaloid. FYN, P. lactiflora ‘Fen Yu Nu’; LT, P. lactiflora ‘Lian Tai’.

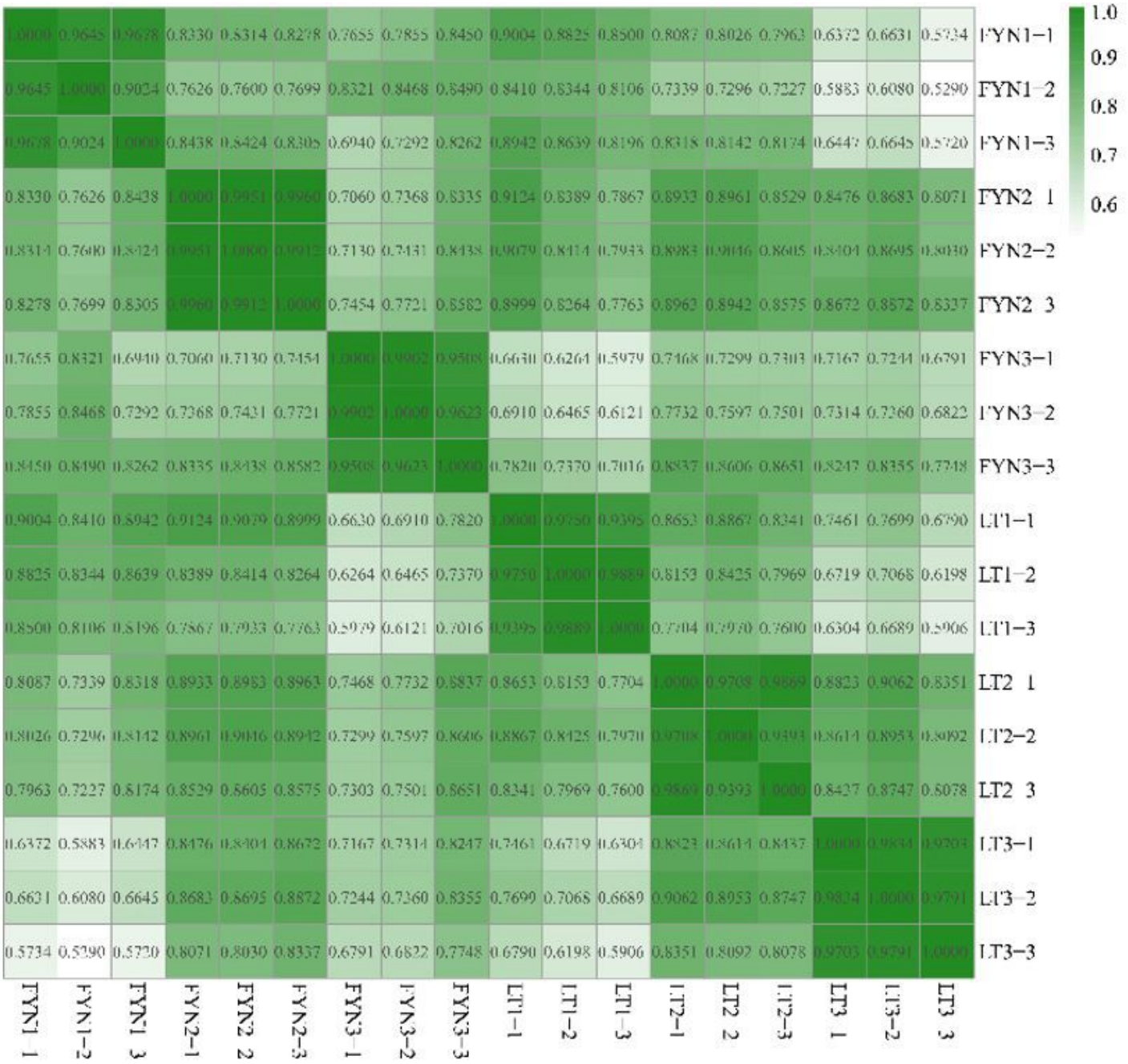

Figure 3

Heatmap of Pearson's correlation between samples. X and Y axes represent samples. FYN1-1, FYN1-2, and FYN1-3 represent three biological repeats of FYN in the stamen primordium period of development; FYN2-1, FYN2-2, and FYN2-3 represent three biological repeats of FYN in the stamen elongation period; FYN3-1, FYN3-2, and FYN3-3 represent three biological repeats of FYN in stamens completed development period; LT1-1, LT1-2, and LT1-3 respectively represent three biological repeats of LT in the stamen primordium period; LT2-1, LT2-2, and LT2-3 represent three biological repeats of LT in the stamen partly petaloid period; LT3-1, LT3-2, and LT3-3 represent three biological repeats of LT in the stamens completed petaloid development. FYN, P. lactiflora 'Fen Yu Nu'; LT, P. lactiflora 'Lian Tai'.

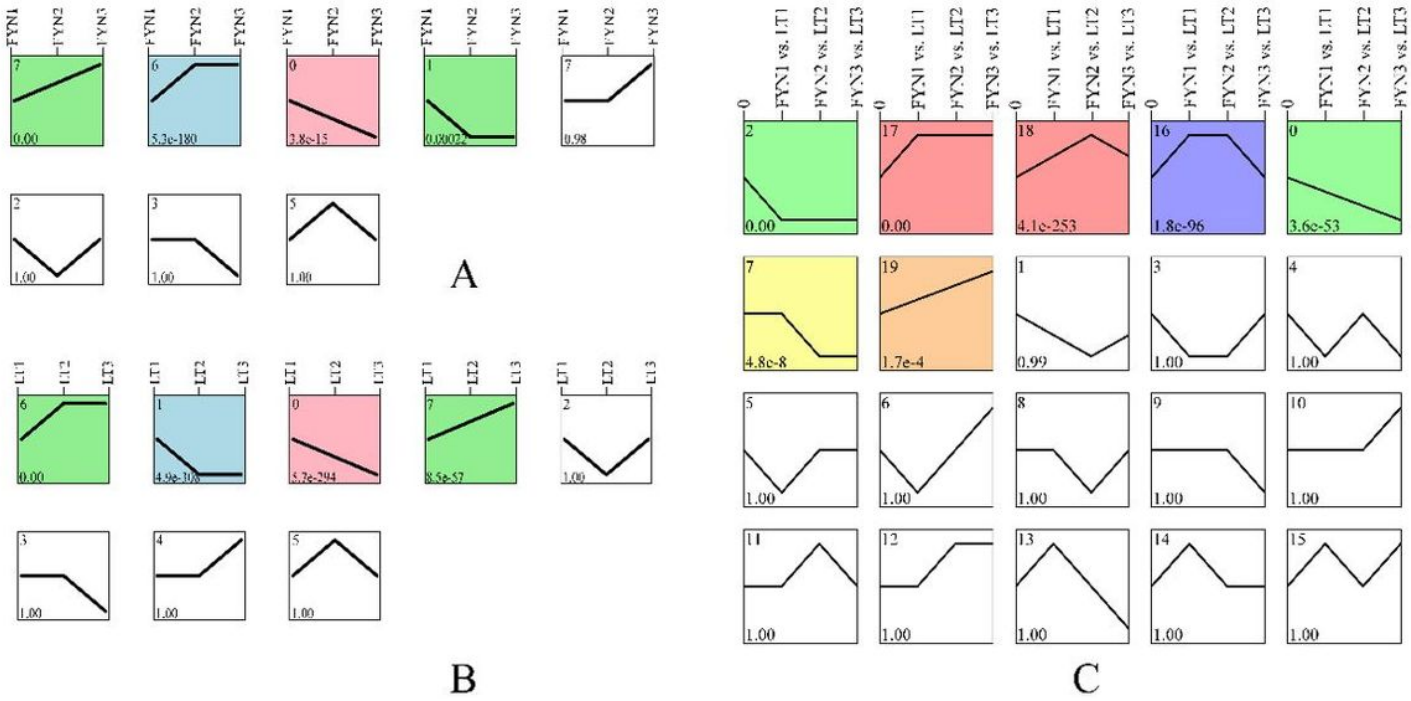

Figure 4

Trend analysis of DEGs. A Trends of FYN gene expression profiles. B Trends of LT gene expression profiles. C Trends of FYN vs. LT gene expression profiles. The X-axis of A and B represent the FYN1-FYN3 and LT1-LT3 periods respectively, and the X-axis of C represents the corresponding periods in the FYN vs. LT comparison. The Y-axis represents the change in gene expression. Numbers in the upper left corner represent the serial number of each trend analysis module and numbers in the lower left corner represent the p value of the trend module. FYN, P. lactiflora ‘Fen Yu Nu’; LT, P. lactiflora ‘Lian Tai’.

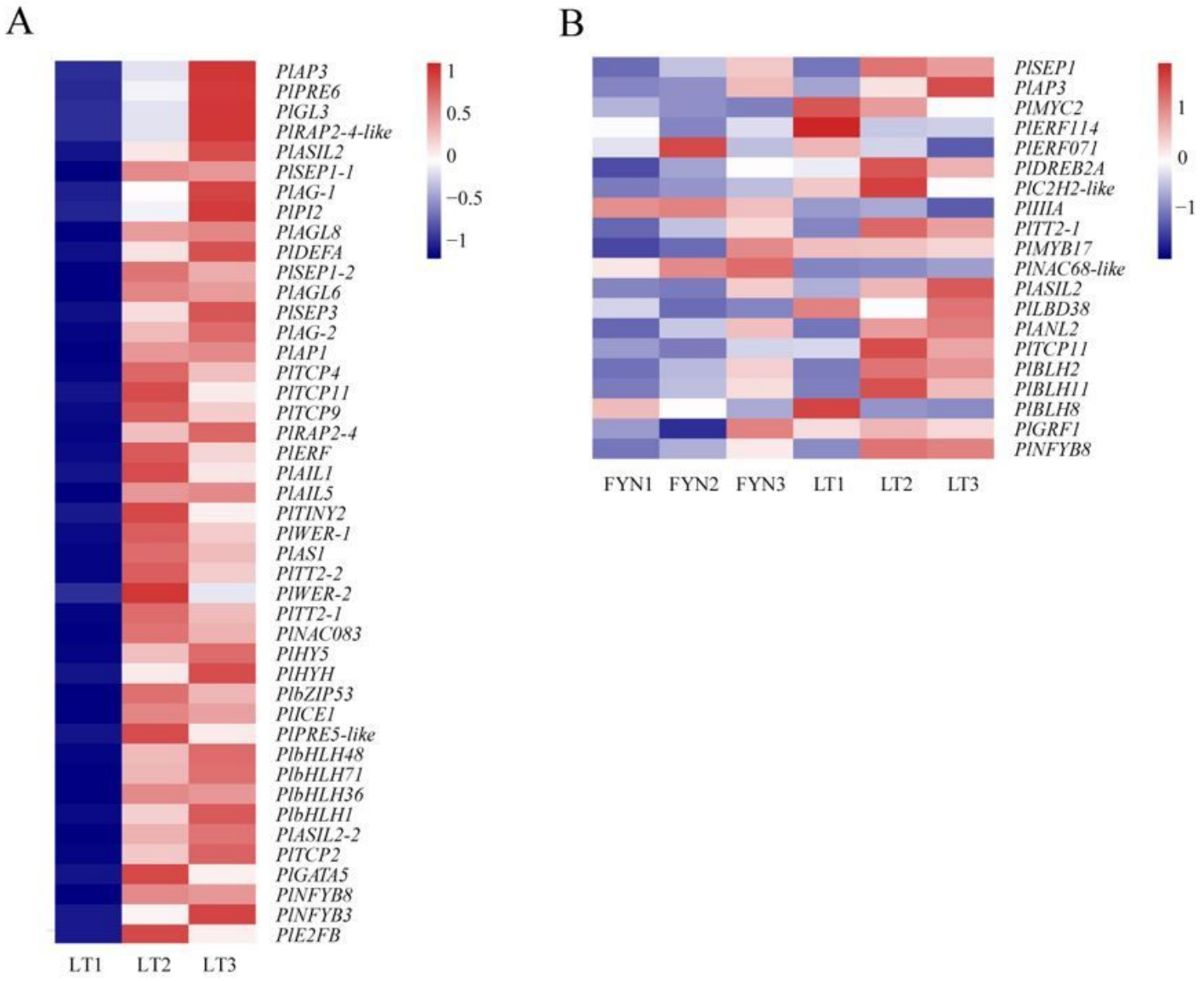

Figure 5

Heatmaps of MADS-box and transcription factor differentially expressed genes (DEGs) in P. lactiflora. (A) Heatmaps of DEGs from profiles 6 and 7 in LT. (B) Heatmaps of DEGs from FYN vs. LT. FYN, P. lactiflora ‘Fen Yu Nu’; LT, P. lactiflora ‘Lian Tai’.

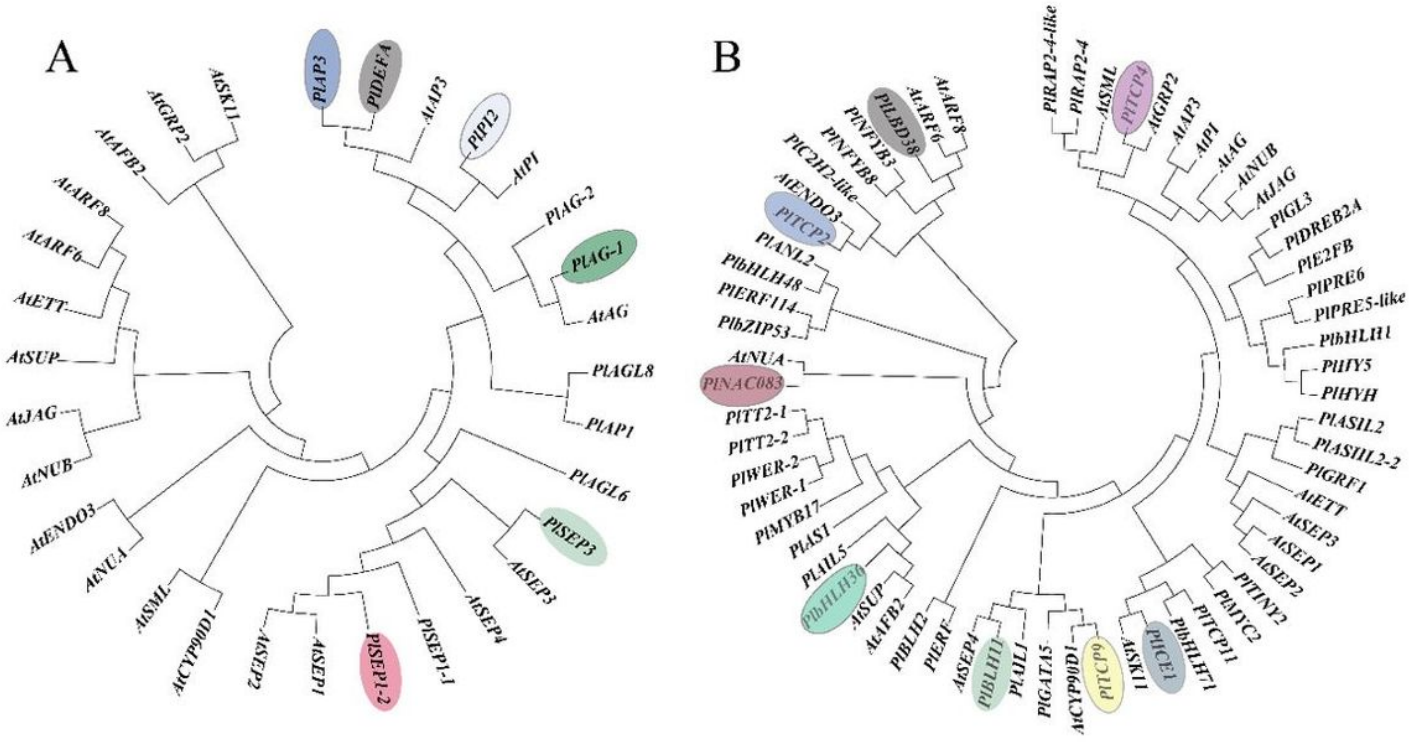

Figure 6

Phylogenetic analysis of differentially expressed genes (DEGs) of MADS-box and TFs from trend analysis of LT profiles and FYN vs. LT combinations that might be related to P. lactiflora petaloid stamens. A Phylogenetic tree between MADS-box DEGs during the development of P. lactiflora and the genes that regulate stamen development in A. thaliana. B Phylogenetic tree between TF DEGs during the development of P. lactiflora and the genes that regulate stamen development in A. thaliana. The genes that regulate stamen development in A. thaliana were downloaded from the NCBI database, and the phylogenetic trees were drawn using EMGA7.

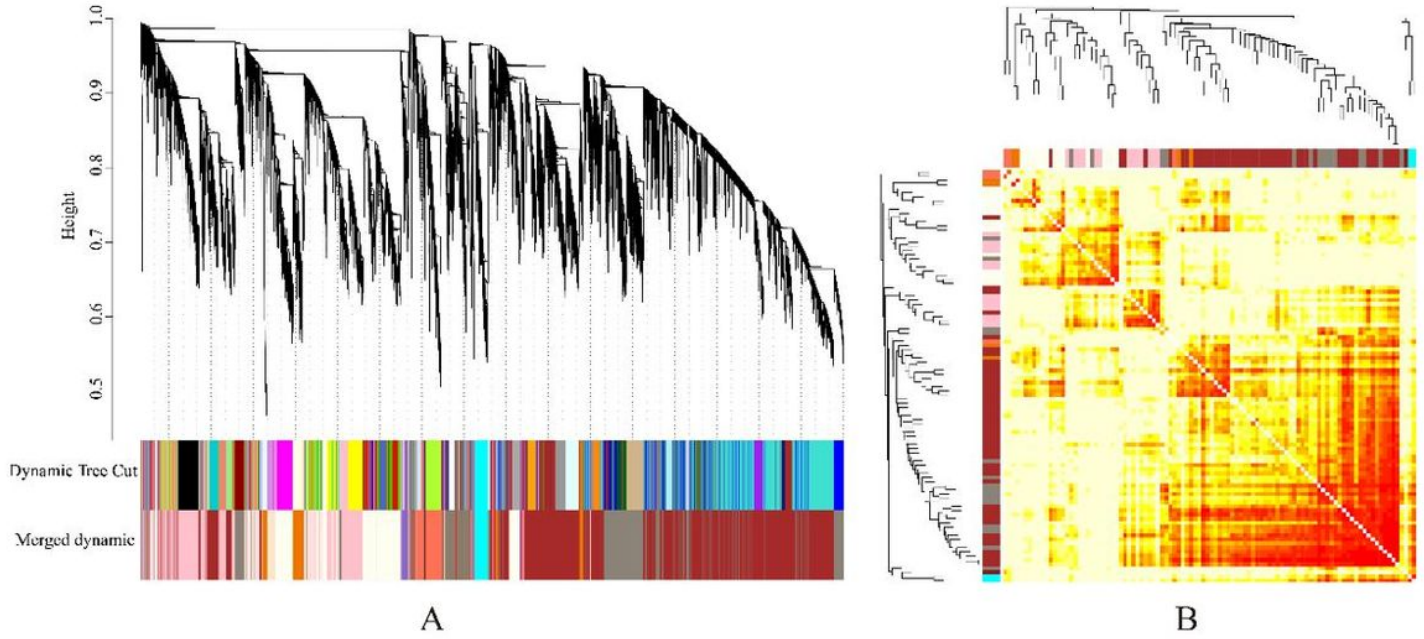

Figure 7

Weighted gene co-expression network in P. lactiflora. A Module-level clustering diagram. Dynamic Tree Cut: gene modules obtained from the dynamic tree cut; different colors represent different modules. Merged dynamic: The merged co-expression modules with a similar expression pattern. The longitudinal distance represents the distance between genes; the horizontal distance is meaningless. B Module gene correlation heatmap. Each row and column represents a gene, and the deeper the color of each dot (white → yellow → red), the stronger the connectivity between the two genes corresponding to the row and column, and the stronger the Pearson's correlation.

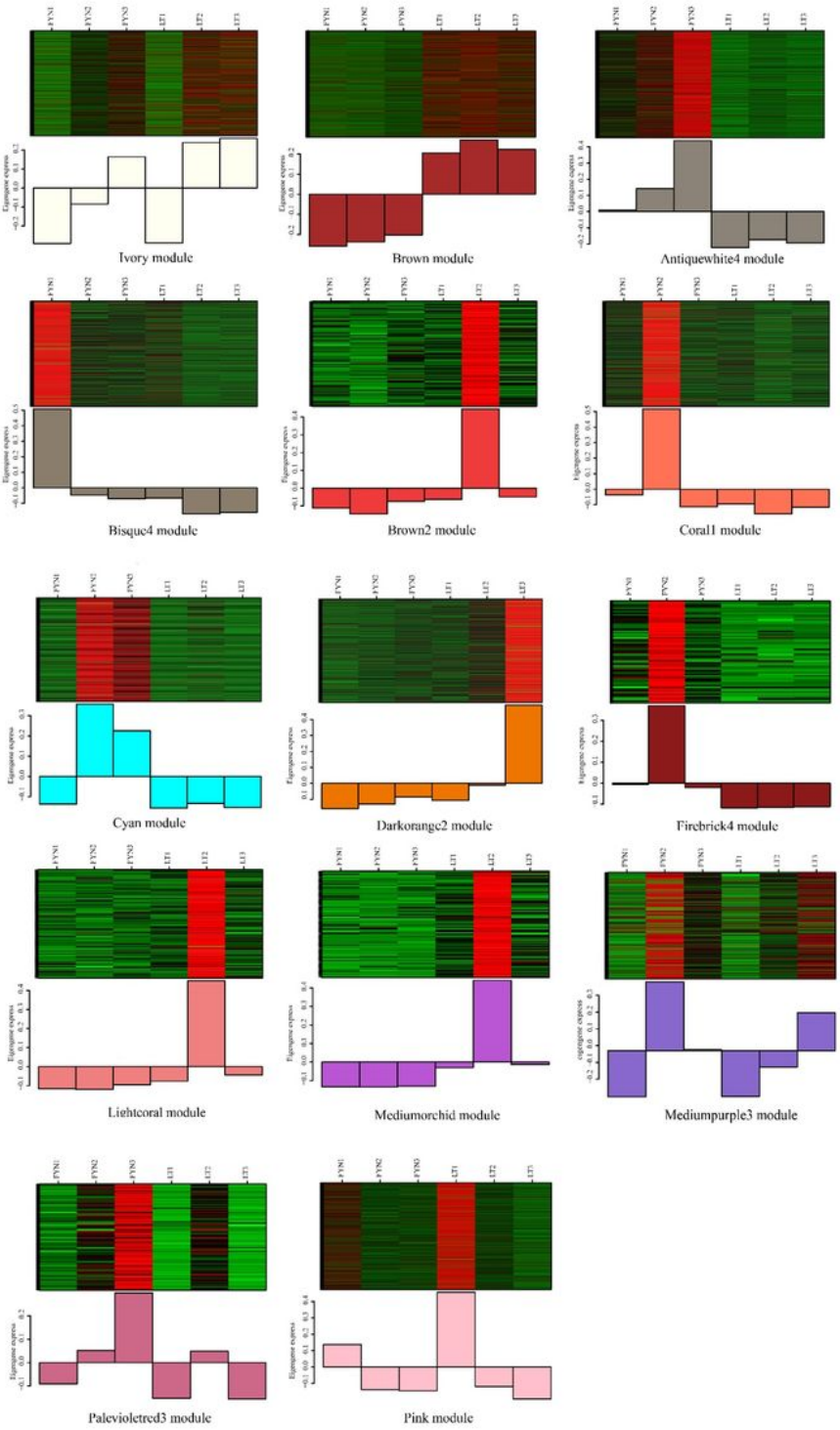

Figure 8

Heatmap of gene expression pattern of each module. The upper part of the figure is a heat map of the gene expression in different samples: red is up-regulation; green is down-regulation; the lower part of the figure is the eigengene value of the gene in different samples. FYN, P. lactiflora ‘Fen Yu Nu’; LT, P. lactiflora ‘Lian Tai’.

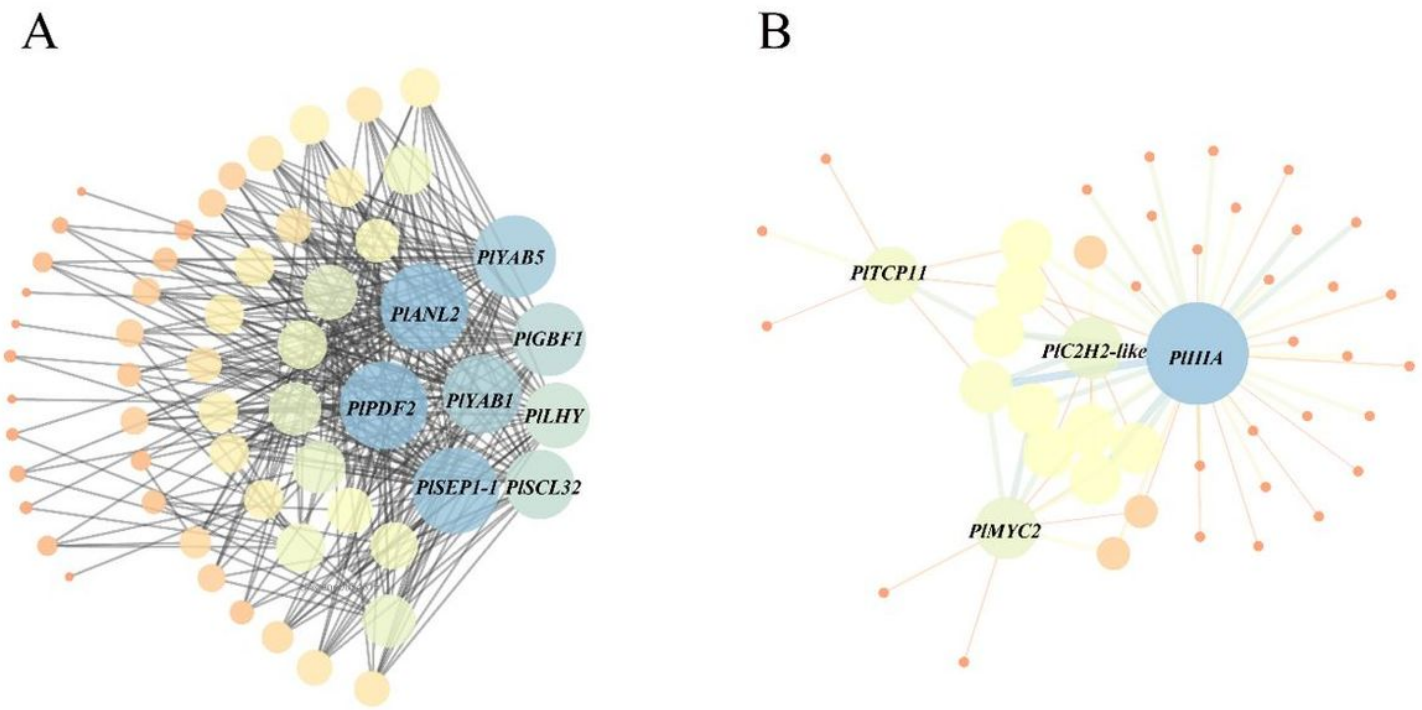

Figure 9

Genes regulation weight network related to petaloid stamens of P. lactiflora (FYN and LT). (A, B) The genes regulation weight network of differentially expressed genes in Ivory and Brown modules, respectively (based on the findings of Fig. 8). Circle size is positively correlated with the interaction strength between genes. Different colors show different connectivities.

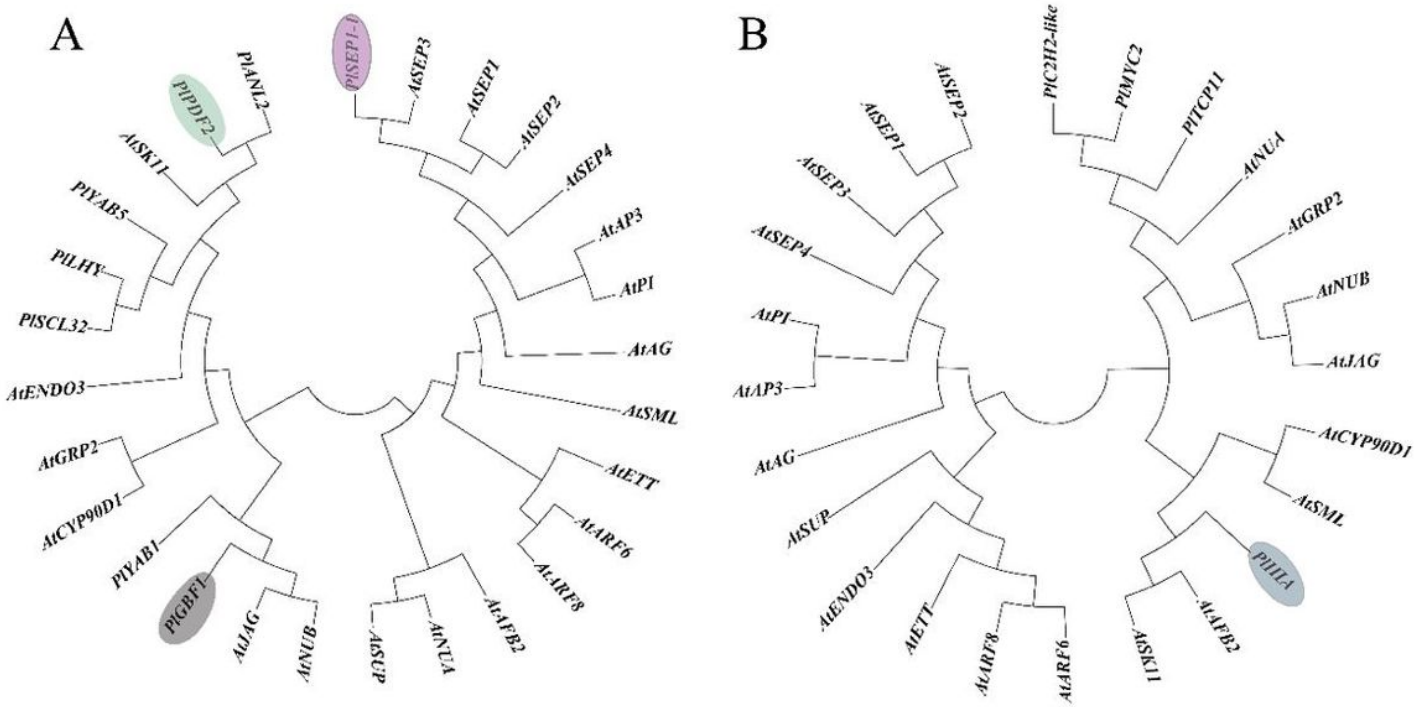

Figure 10

Phylogenetic analysis of differentially expressed genes (DEGs) in Ivory (A) and Brown (B) modules. Phylogenetic trees between DEGs in the Ivory (A) and Brown (B) modules and the genes that regulate stamen development in A. thaliana. The genes that regulate stamen development in A. thaliana were downloaded from the NCBI database, and the phylogenetic trees were drawn using EMGA7.

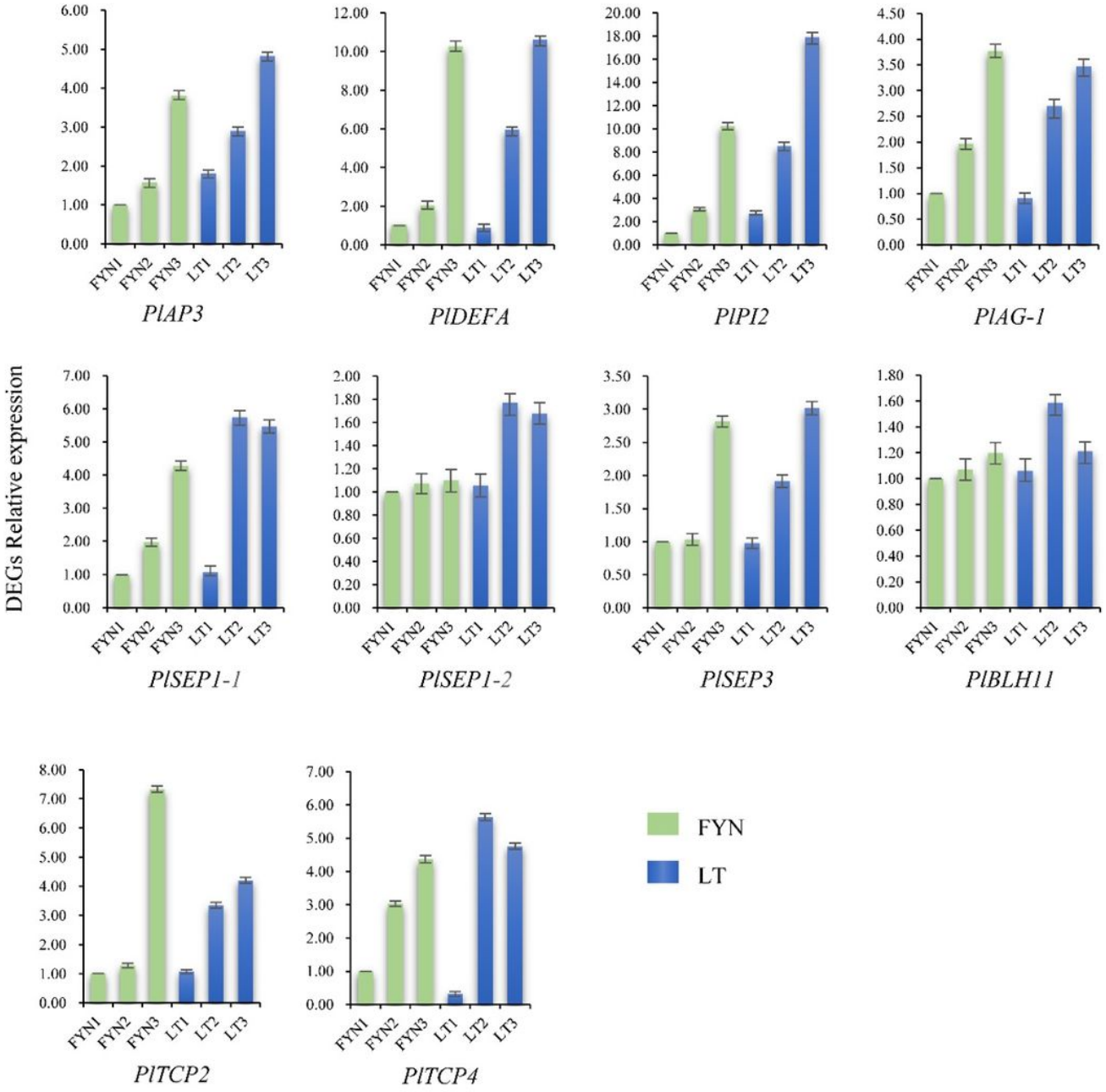

Figure 11

Validation of RNA-Seq results by qRT-PCR. Green bars show the expression of FYN1-3. Blue bars show the expression of LT1-5. Y-axis: relative expression level of differentially expressed genes (DEGs). FYN, P.

lactiflora ‘Fen Yu Nu’; LT, P. lactiflora ‘Lian Tai’.

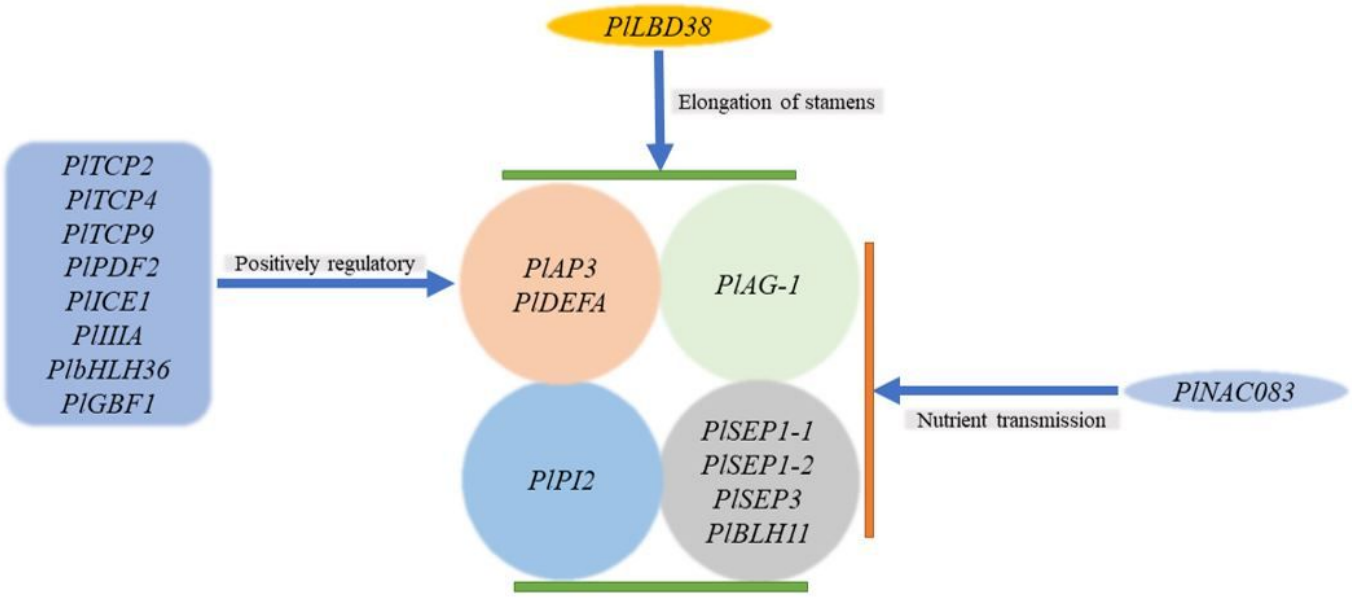

Figure 12

Inference model of gene regulatory network for P. lactiflora petaloid stamens.

Supplementary Files

This is a list of supplementary files associated with this preprint. Click to download.

- Additionalfile9.xlsx
- Additionalfile8.xlsx
- Additionalfile7.png
- Additionalfile6.xlsx
- Additionalfile5.xlsx
- Additionalfile4.png
- Additionalfile3.xlsx
- Additionalfile2.png
- Additionalfile1.xlsx